Processing-Dependent High Impact Polystyrene/Styrene-Butadiene-Styrene Tri-Block Copolymer/Carbon Black Antistatic Composites

Weihua Tang,[1] Beibei Liu,[1] Zhiwei Liu,[2] Jian Tang,[1] Huilin Yuan[2]

[1]*Key Laboratory of Soft Chemistry and Functional Materials, Ministry of Education of China, Nanjing University of Science and Technology, Nanjing 210094, China*
[2]*Beijing Key Laboratory of Novel Polymer Materials Preparation and Processing, Beijing University of Chemical Technology, Beijing 100029, China*

Received 19 November 2010; accepted 24 March 2011
DOI 10.1002/app.34559
Published online 9 August 2011 in Wiley Online Library (wileyonlinelibrary.com).

ABSTRACT: The electrical resistivity and morphology of high impact polystyrene (HIPS)/styrene-butadiene-styrene triblock copolymer (SBS)/carbon black (CB) blends were studied. Their antistatic sheets were prepared by both compression-molding and extrusion calendaring process, with their surface morphology observed using scanning electron microscopy (SEM). The SEM images reveal better dispersion of CB achieved in extrusion-calendering, resulting in low percolation threshold values in HIPS composites. Higher compression ratio and higher drawing speed (corresponding lower sheet thickness) are beneficial to get better CB dispersion, leading to decreased conductivity for the antistatic sheets. SEM images indicate that strong shear forces in extrusion tend to break the conductive network of CB, resulting in increased surface resistivity. © 2011 Wiley Periodicals, Inc. J Appl Polym Sci 123: 1032–1039, 2012

Key words: polymer-matrix composites; electrical properties; compression molding; extrusion

INTRODUCTION

Most polymers are thermally and electrically insulating in nature. Their derived packaging materials can easily accumulate static charge during manufacturing, assembling, storage, and service. The electrostatic discharge (ESD) of the packaging materials often causes damage to the electronic components stored inside, with annual losses estimated in billions of dollars.[1–3] Therefore, the electronic industry association (EIA) and the electrostatic discharge association (ESDA) have established international standards demanding ESD protection for sensitive electronic devices.[4] The antistatic packaging materials are generally prepared by blending polymer matrix with conductive polymers or fillers, allowing creating new polymeric materials with unique electrical properties.[5–18] For antistatic application, the magnitude of the volume electrical resistivity of packaging materials ranges from 10^5 to 10^{14} Ω cm.[7]

The approach by blending engineering polymers with conductive fillers is widely used due to variable conductive fillers, feasible melt-mixing processing, and controllable resistivity. For a given polymer composites, electrical conductivity is strongly dependent upon the amount, type, and shape of the conductive fillers.[1,9] The critical content of conductive fillers necessary to initiate a continuous conductive network is refereed to as the percolation threshold, which varies from polymer to polymer for a given type of fillers. A plateau of resistivity is generally reached with a small increase of filler concentration after the percolation threshold.[19] Carbon black (CB) filled polymer composites are the most widely used antistatic systems for packaging applications,[7,20] with a general CB loading between 15 and 20% by weight.[7,9] This relatively high CB concentration causes local difference of CB concentration, resulting in variation of the conductivity with location in the same product. It is imaginable that the conductivity of CB-loaded polymer composites is closely related with CB content, composite morphology, and CB location within the composites.[4,8,11,12]

As a widely used packaging material, high impact polystyrene (HIPS) possesses excellent mechanical

Correspondence to: W. Tang (whtang@mail.njust.edu.cn) or H. Yuan (yuanhuil@263.net).

Contract grant sponsor: Nanjing University of Science and Technology.
Contract grant sponsor: National Natural Science Foundation of China; contract grant number: 21074055.
Contract grant sponsor: Foundation of Key Laboratory of Luminescence and Optical Information; contract grant number: 2010LOI04.
Contract grant sponsor: NUST Research Funding; contract grant number: 2010ZDJH04.

properties, good coloring capability, and feasible processability. However, its applications are often limited by its relatively low impact strength, heat deflection, and flame retardancy.[21] Solutions in toughening HIPS with rubber, elastomer, or polymer alloy will inevitably sacrifice its stiffness.[22,23] Inorganic nanoparticles toughening approaches, however, can afford polymer composites with good balance of mechanical performance, i.e., higher rigidity and improved toughness at the same time. CB particles are widely used as a reinforcing filler to improve dimensional stability, a conductive filler to dissipate static charge, and an UV-light stabilizer/oxidant to prolong rubber lifetime. Along this direction, CB or ZnO nanoparticles loaded antistatic packaging materials have been reported with a good combination of mechanical performance: styrene-isoprene-styrene (SIS) toughened HIPS/SIS/CB composites (CB loading $\sim$ 5 wt %),[24] ZnO-reinforced PS/ZnO nanocomposites,[14] and CB-filled polyethylene/ethylene vinyl acetate/CB.[25] In comparison to CB, larger amount of ZnO is needed to prepare antistatic PS/ZnO composites, e.g., 30 wt % addition of spherical ZnO decreasing the surface resistivity from 1.0×10^{16} to 8.98×10^{12} $\Omega\,cm^{-2}$.

In this study, SBS-toughened HIPS/SBS/CB antistatic composites were prepared by both compression molding and extrusion calendaring. The correlation of surface resistivity of the resulting antistatic sheets with CB loading, processing approaches, and processing parameters was studied in detail. The morphology of antistatic sheets achieved with different processing approaches was also discussed.

EXPERIMENTAL

Materials

Commercial grade of HIPS (HI 410T) with 7.5 g/10 min melt flow index (MFI) (at 200°C under 5 kg load) was supplied by KUMHO Petrochemical Co. (Korea). SBS (YH-796) with a polystyrene content of 25 wt % and MFI of 2.3 g/10 min (at 230°C under 2.16 kg load) was procured from Baling Petrochemical Co. Ltd. (SINOPEC, China). CB (V-XC72) (Cabot Co., Boston, MA) was used in this study.

Preparation of antistatic sheets

The HIPS/SBS/CB antistatic sheets were prepared by either compression molding or extrusion calendaring (fabrication flowchart shown in Fig. 1). The HIPS/CB, HIPS/SBS/CB polymer composites were prepared by melt-mixing oven-dried HIPS and CB or HIPS, SBS and CB according to designed formulation in a corotating twin-screw extruder (Φ20, $L/D = 40$) (Kunshan Kexin rubber and plastic machine, China) at a speed of 90 rpm at 190°C. The HIPS/SBS*/CB composites were prepared by melt-mixing HIPS/SBS master batch (HIPS/SBS*) with CB. The extrudates were further pelletized and dried at 100°C for 6 h. For compression molding processing, the antistatic sheets (thickness: 0.4, 0.6, or 1 mm) were fabricated with a plate vulcanizer at 190°C. For extrusion and calendering processing, the dried antistatic pellets were further melt-blended in a single-screw extruder (PLD-651, Φ30, $L/D = 25$) (Brabender, Germany) and calendered with a three-roll calender (Φ120×200) (Brabender, Germany) to obtain the antistatic sheets.

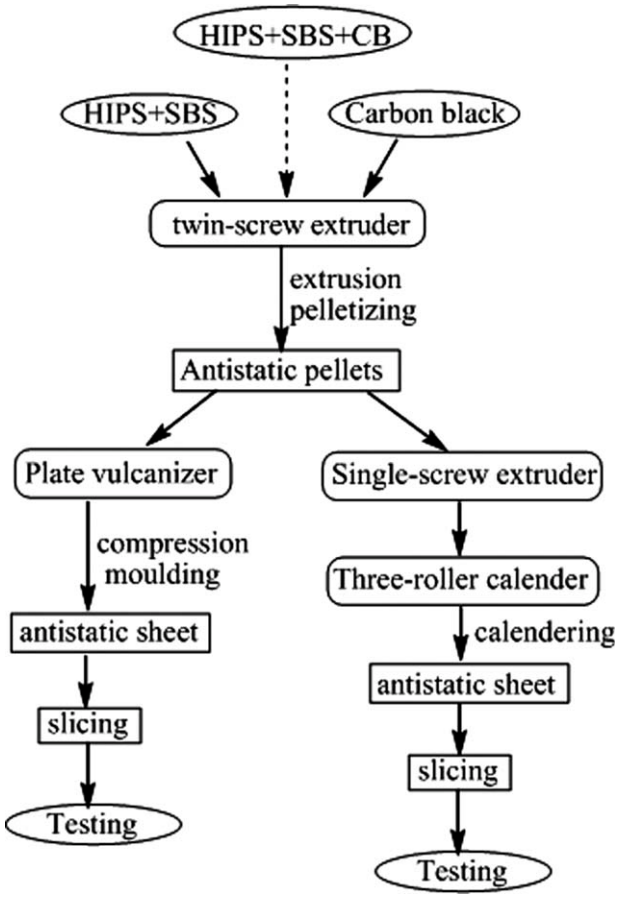

Figure 1 Flowchart of composite fabrication via compression-molding and extrusion-calendering.

Characterization

The surface resistivity of sheet samples was measured in the thickness direction using ZC-90 high resistance electrometer (Yuanzhong Electronic Instrument Co. Shanghai, China) with a measurement range of 1.0×10^4 Ω to 2.0×10^{13} Ω, according to standard GB 1410-89. The blends' phase morphology was examined using an *S*-4700 (Hitachi, Japan) scanning electron microscope (SEM). The samples were sputter-coated with a thin layer of gold before examination with SEM.

RESULTS AND DISCUSSION

Influence of processing methods on surface resistivity

For the preparation of antistatic packaging materials, a CB loading of 10–20% is often needed.[7,9] This relatively high CB concentration brings negative effect on the processability of the polymer composites and their mechanical properties. To improve the impact strength of PS, SBS was used herein as toughening agent for PS/CB composites due to its high compatibility with PS.[4] Supertoughened HIPS/SBS blends with Izod impact strength $\geq$500 J m^{-1} can be achieved when fixing the weight ratio of HIPS to SBS as 100/40.[22,23,26,27] HIPS/SBS (100/40) blends were thus selected to investigate the effect of CB loading on the conductivity of HIPS/CB, HIPS/SBS/CB, and HIPS/SBS*/CB composites prepared with different processing approaches. As shown in Figure 1, the CB-loaded HIPS antistatic materials were prepared by either compression molding or extrusion calendaring of melt-mixed HIPS/CB, HIPS/SBS/CB, or HIPS/SBS*/CB composites.

The surface resistivity for the extrusion-calendered antistatic sheets with the thickness of 1 mm varied with CB loading (Fig. 2). With 10% CB, HIPS-based composites exhibit high surface resistivity in the magnitude of 10^{14} Ω cm and SBS-toughened HIPS composites present slightly better conductivity. Increasing CB loading to 15%, HIPS/CB compounds only shows one order of magnitude decrease in surface resistivity, while HIPS/SBS/CB (100/40/15) composites exhibit seven orders of magnitude lower surface resistivity than HIPS/SBS/CB (100/40/10). This significant reduction in resistivity for HIPS/SBS/CB composites indicates that the percolation value of CB in HIPS/SBS blends lies between 10 and 15%. However, the percolation value of CB for HIPS/CB compound should be higher than 15%. As well-established now, the selective distribution of conductive fillers like CB in polymer composites can be predicted using Young's equation[28] as below.

$$\gamma_{CB-\alpha} + \gamma_{\alpha-\beta}\cos\theta = \gamma_{CB-\beta}, \quad (1)$$

$$w_a = \frac{\gamma_{CB-\beta} - \gamma_{CB-\alpha}}{\gamma_{\alpha-\beta}}, \quad (2)$$

where $\gamma_{CB\text{-}\alpha}$, $\gamma_{CB\text{-}\beta}$, and $\gamma_{\alpha\text{-}\beta}$ are the interfacial tension between component CB and α-polymer, between CB and β-polymer, and between α- and β-polymer, respectively; θ is the contact angle of the polymer on the CB; w_a is the wetting coefficient. If $w_a > 0$, that is, $\gamma_{CB\text{-}\beta} > \gamma_{CB\text{-}\alpha}$, CB particles will distribute overwhelmingly in α-polymer or at the interfaces. Otherwise, CB particles will dominantly distribute in β-polymer or at the interface.

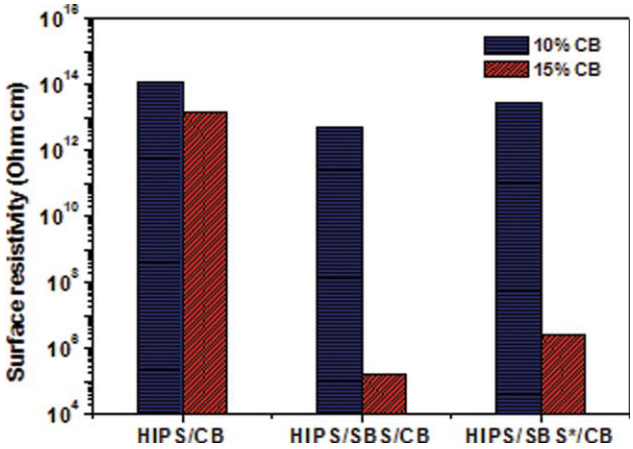

Figure 2 The surface resistivity (ρ_s, Ω cm) of HIPS-based antistatic sheets (thickness, 1 mm) with different CB loading via calendaring technique. [Color figure can be viewed in the online issue, which is available at wileyonlinelibrary.com.]

According to the empirical data of PS and CB[21] and calculation of Sundararaj and coworker[4] the interfacial tension between PS and CB is 36.5 mN m^{-1}, which is slightly higher than that between polybutadiene (PBD) and CB (35.8 mN m^{-1}).[4] As known to all, the surface tension of copolymer is always lower than that corresponding to the component of higher surface tension, even if this component is present in relatively small amounts. In our case, PS (γ = 27.7 mN m^{-1})[29] is the component with higher surface tension for both polymers: HIPS and SBS, while butadiene rubber (PBD) (γ = 22.7 mN m^{-1}).[29] It is possible to assume that the weighted surface tension of HIPS is closer to that of PS than the weighted surface tension of SBS. Therefore, the interfacial interactions between HIPS and CB will be higher than that between SBS and CB following Mohammed and Sundararaj's calculation.[4] Hence, CB particles have a very high probability of dispersion in SBS phase or at the interfaces between HIPS and SBS.

For the particular SBS triblock copolymer structure, it was found that PS domains of SBS are of spherical shape.[8] In the study of HIPS/SIS/CB composite, Tchoudakov et al. also observed the preferential localization of CB particles in PS rather than in SIS and explained this phenomenon with a model.[8] According to this model, the first CB particles, incorporated into SBS, are engulfed by PS domains. These CB encapsulated by PS does not contribute to the material's conductivity. The subsequently added CB particles saturate most of PS domains in SBS, and excess CB starts to form segregated CB morphology. Only when the CB percolation within SBS is exceeded, a conductive CB network is formed through the two-phase SBS medium.

In this study, HIPS has a minor component, butadiene rubber less than 10%, where 25% PS exits in SBS as the minor component. Compared with HIPS/CB, HIPS/SBS/CB and HIPS/SBS*/CB blends studied in our study, since CB has a priority to saturate PS domains in SBS phase and segregates to form conductive network in the presence of excess CB, HIPS/SBS/CB and HIPS/SBS*/CB blends should achieve conductive network at lower CB addition, i.e., lower CB percolation is present in SBS-toughened HIPS blends. This is in agreement with the results observed in Figure 2.

The electrical properties of HIPS/CB, HIPS/SBS, HIPS/SBS*/CB composites prepared by compression molding are shown in Figure 3. Compared with those composites fabricated by extrusion calendaring, the corresponding composites present much higher conductivity. Importantly, the percolation threshold values of CB fall between 10 and 15% for all composites. This phenomenon can be explained by the surface enrichment of component with lower interfacial tension. As discussed earlier, HIPS-CB system has a higher interfacial tension than SBS-CB system, CB tends to have higher affinity with SBS. When SBS enriches in the surface of HIPS/SBS/CB composites, more CB localizes in PS domains in the surface area. Therefore, the surface resistivity of SBS-toughened HIPS systems exhibits almost eight orders of magnitude reduction as compared with HIPS/CB composite. However, by extrusion-calendering process, since SBS is highly compatible with HIPS, a second melt-mixing by extrusion results in better dispersion of SBS into HIPS phase. The conductive network of CB, hence, is more difficult to form in these higher separated PS domains after increased melt-mixing processes.[7] The same behavior is observed in the premixed HIPS/SBS*/CB composites, twice-mixed composites provide better dispersion of SBS in HIPS matrix, which causes four times lower surface conductivity than that of HIPS/SBS/CB composite.

The localization of CB in HIPS/SBS/CB composites can be investigated with their surface morphology. Figure 4 shows the SEM images of 10% CB-loaded HIPS/SBS/CB antistatic HIPS sheets (thickness, 1 mm). Typical island-sea morphology is observed with HIPS as the gray continuous phase and SBS as white dispersed phase. Since CB particles first saturate PS domains of SBS and aggregate when excess CB is added. In this case, CB agglomerates can form around lighter SBS phase. The brighter SBS particles (pointed by red arrows, size 0.1–0.4 μm) as island disperse in HIPS gray sea; while light CB particles disperse as tiny particles either in HIPS phase (circle zone) or SBS particle surface (square zone) or aggregated in matrix (oval zone, 0.1 μm size). The localization of CB in either HIPS matrix or SBS dispersed phases is schematically shown as the bottom panel in Figure 4(c).

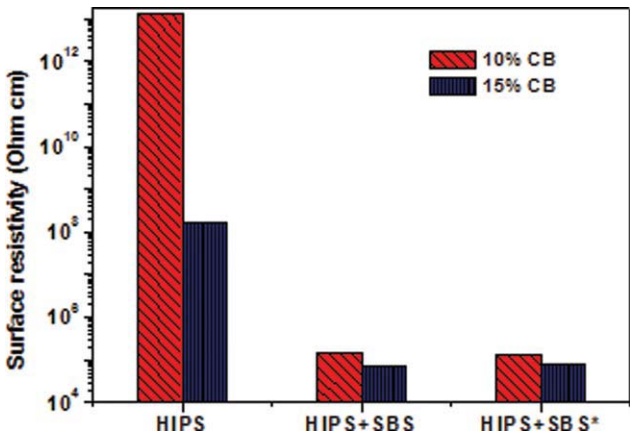

Figure 3 The surface resistivity of HIPS-derived antistatic sheets (1 mm) prepared with compression molding. [Color figure can be viewed in the online issue, which is available at wileyonlinelibrary.com.]

The effect of re-blending times

As discussed earlier, extrusion calendering processing achieves better SBS dispersion in continuous HIPS phase than compression molding, indicating that the shear force during melt-mixing is beneficial for dispersion of SBS. Herein, we investigate the effect of blending time on the electrical properties of HIPS/CB(15%) composites. The experiments were conducted by repeating melt-blending of HIPS/CB pellets in twin-screw extruder prior to the final extrusion-calendering to prepare antistatic sheets. The effect of re-blending times on the surface resistivity is shown in Figure 5. A Poisson distribution type curve of surface resistivity is observed when increasing the re-blending times. The maximum surface resistivity is achieved with twice re-blending of HIPS/CB composites. This behavior can be explained by SBS dispersion with increased melt-mixing time.

According to Boonstra and Medalia,[30] polymer firstly penetrates into the interstices between CB particles during the early stage of melt-mixing, the maximum amount of penetrated polymer is determined by the CB void volume. And the weak Van der Waals forces between CB particles make them easily broken up. The formation of CB conductive network is strongly dependent on dispersion of SBS and CB content. With the increasing re-blending, SBS achieved better dispersion in HIPS composites. It is possible that the resistivity increases with the mixing time when SBS achieved increased dispersion and CB aggregates gradually breakup in the initial formation stage of conductive network. After the breakup of CB aggregates completed ($\sim$ 2 re-blending) and SBS

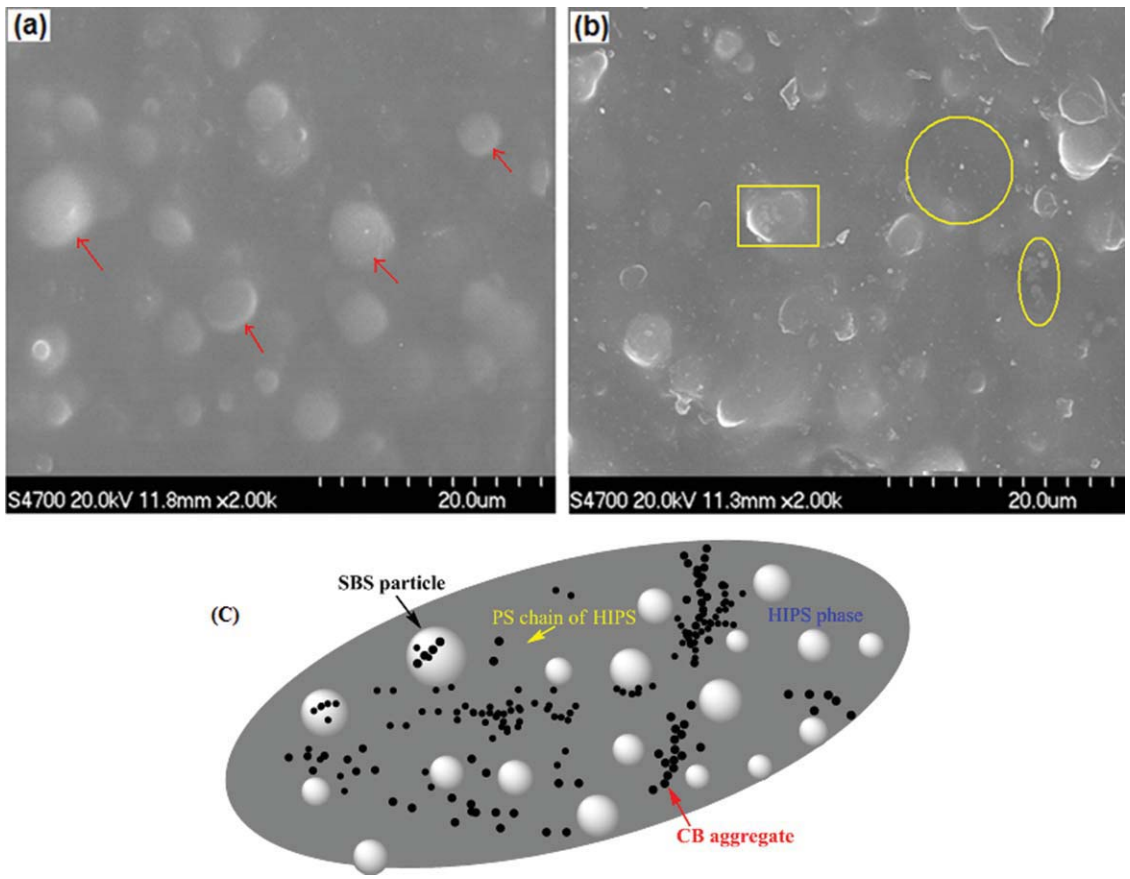

Figure 4 SEM micrographs of HIPS/SBS/CB(10%) antistatic sheet surface by (a) extrusion-calendering and (b) compression-molding. Brighter SBS particles (pointed by red arrows, size 0.1–0.4 μm) as island disperse in HIPS gray sea; while CB particles disperse as tiny particles either in HIPS phase (circle zone) or SBS particle surface (square zone) or aggregated in matrix (oval zone). A schematic localization of CB is shown as the bottom panel (c). [Color figure can be viewed in the online issue, which is available at wileyonlinelibrary.com.]

dispersion reaches its optimum, the conductivity of this composite reaches its minimum due to incomplete conductive network.[7] Further re-blending the HIPS/CB composites, the conductivity of materials increases with the increased coalesce of well-dispersed SBS and CB aggregates, which is beneficial for the formation of conductive network. In conclusion, two re-blending process

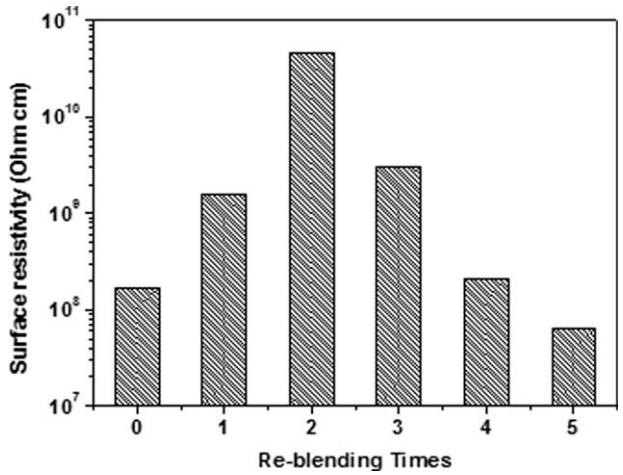

Figure 5 The variation of surface resistivity with re-blending times.

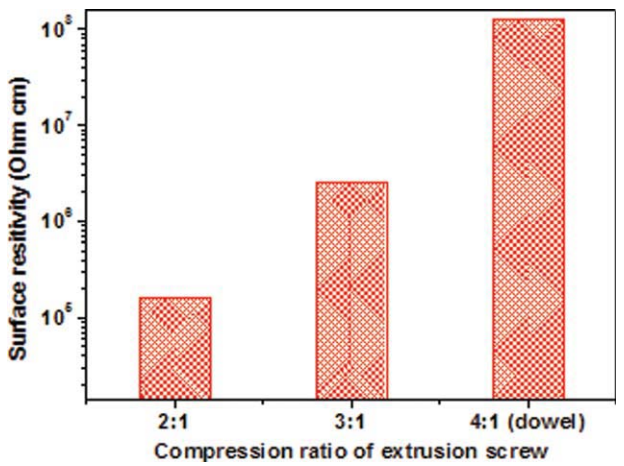

Figure 6 The variation of surface resistivity with the compression ratio of extrusion screw. At compression ratio 4 : 1, the screw was also equipped with dowel for better mixing. [Color figure can be viewed in the online issue, which is available at wileyonlinelibrary.com.]

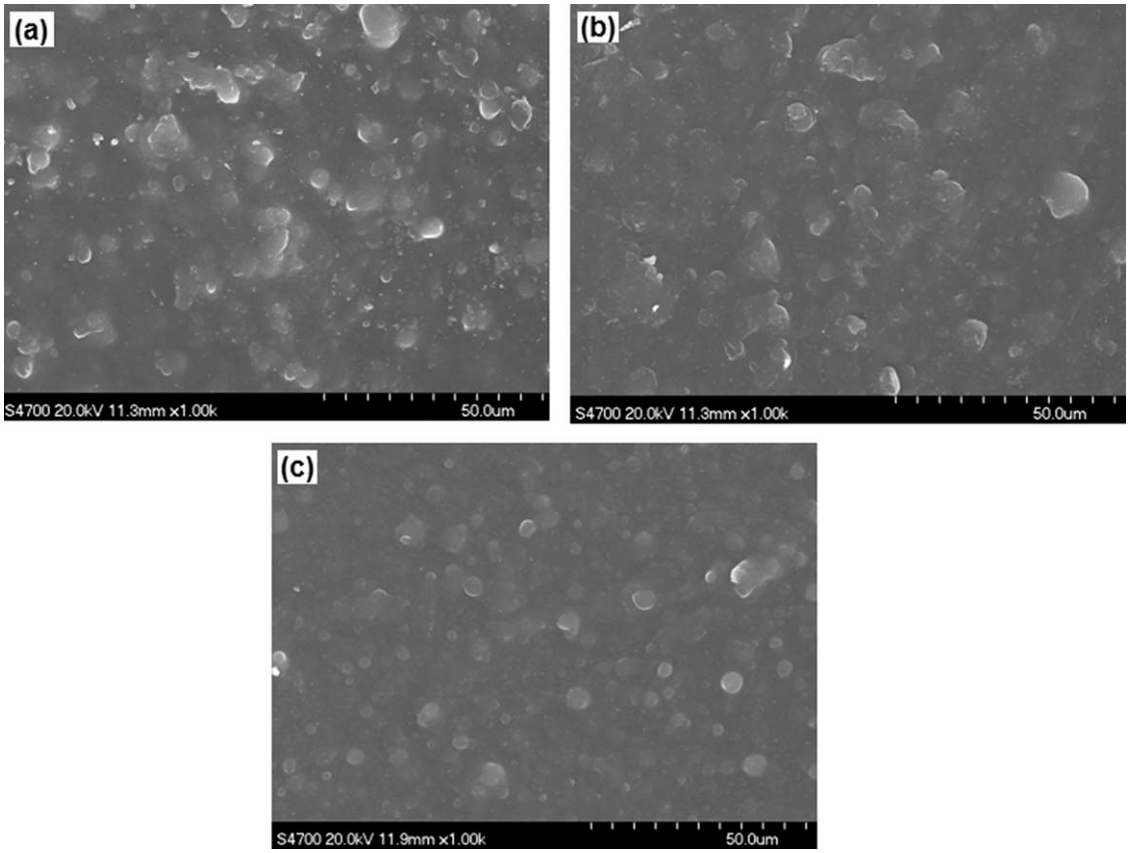

Figure 7 SEM micrographs of HIPS/SBS/CB(15%) antistatic sheets prepared with different compression ratios of extrusion screw (a) 2 : 1, (b) 3 : 1, and (c) 4 : 1.

results in the highest dispersion of SBS in HIPS and complete breakup of CB aggregates, which is undesirable for conductive application. In practical preparation of antistatic material, the perfect dispersion of SBS must be avoided by choosing suitable re-blending times.

The effect of compression ratio of extrusion screw

As discussed above, extrusion-calendering process is more feasible to achieve percolation of CB in HIPS composites than compression molding. It is also known that less mixing is necessary to maintain good dispersion of SBS in HIPS with low CB addition. According to the mixing study by Doonenberg,[31] the conductivity of CB composites decreased with longer mixing time. Hence, efficient control of melt-mixing process is crucial in achieving desired antistatic composites. We thus investigate the effect of screw compress ratio on the surface resistivity of HIPS/SBS/CB(15%) composites.

As shown in Figure 6, we adopted three compression ratios for the sing-screw extruder in the study and a dowel was also equipped at compression ratio 4 : 1. As expected, the surface resistivity of composites increases with higher compression ratio of screw since better dispersion of SBS is achieved due to higher shear forces from screw. The surface resistivity of HIPS/SBS/CB(15%) is 1.6 $\times$ 10^5 Ωcm, 2.5 $\times$ 10^6 Ωcm, and 1.3 $\times$ 10^8 Ωcm, respectively, corresponding to compression ratio 2 : 1, 3 : 1, and 4 : 1.

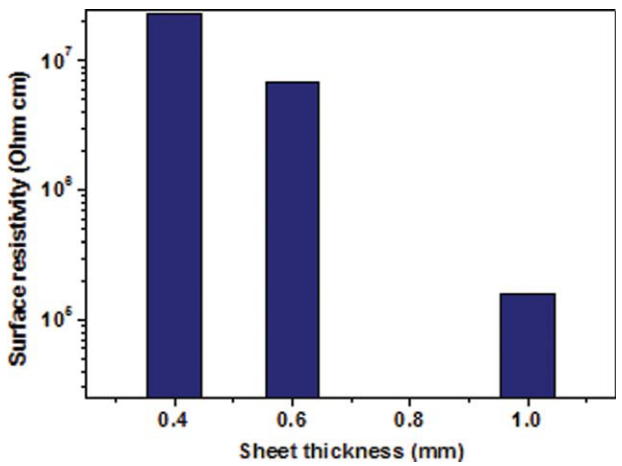

Figure 8 The thickness-dependent surface resistivity of HIPS/SBS/CB(15%) antistatic sheets prepared by extrusion and three-roller calendaring. [Color figure can be viewed in the online issue, which is available at wileyonlinelibrary.com.]

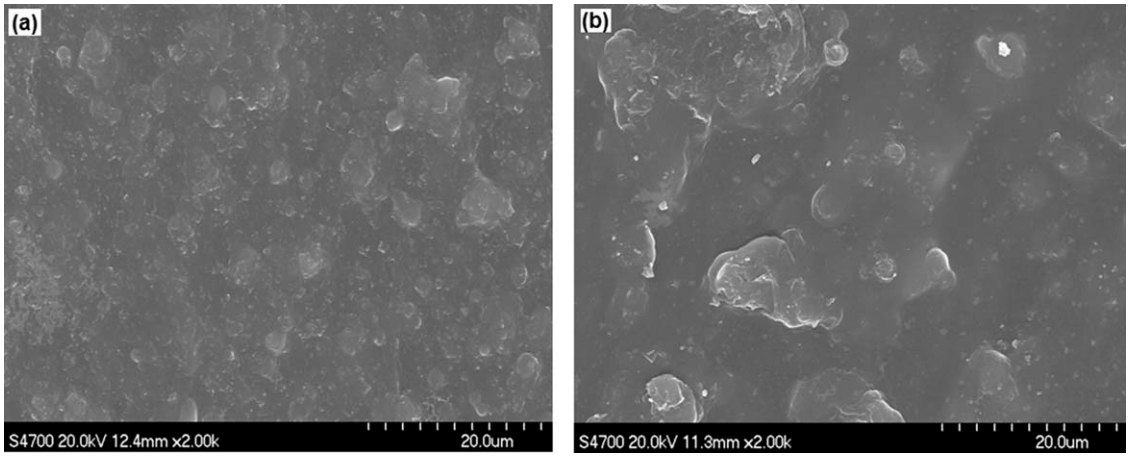

Figure 9 SEM micrographs of HIPS/SBS/CB(15%) antistatic sheets with a thickness of (a) 0.4 mm and (b) 1 mm.

The morphology of HIPS/SBS/CB(15%) composites prepared with different compression ratio is shown in Figure 7. Better dispersion of SBS particles is achieved with higher compression ratio of screw. Smoother surface is also observed in composites prepared with higher compression ratio. At high compression ratio, the distance between CB conductive networks increases and surface enrichment of resin occurs. This can be explained by the increased shear force at higher compression ratio. CB conductive chains were broken near flow channel walls at high shear force, leading to decreased conductivity.

The effect of sheet thickness

In the extrusion-calendering process, the thickness of antistatic sheets can be controlled by the extrusion speed of the single-screw extruder and the drawing speed of the three-roller calender. As known to all, high drawing speed can deform or even destroy the conductive network of CB. Hence, the conductivity of antistatic sheets decreases with higher drawing speed. As imaged, the surface resistivity of HIPS/SBS/CB(15%) decreases at lower drawing speed, corresponding to higher thickness of antistatic sheets (Fig. 8). The surface resistivity of antistatic sheets is $2.3 \times 10^7\ \Omega$ cm, $6.8 \times 10^6\ \Omega$ cm, and $1.6 \times 10^5\ \Omega$ cm, respectively, corresponding to sheet thickness of 0.4 mm, 0.6 mm, and 1 mm.

The surface morphology of HIPS/SBS/CB(15%) antistatic sheet with different thickness is shown in Figure 9. For 0.4-mm thick sheet, more homogenous morphology is observed with smooth surface. The distance between CB conductive networks is enlarged, leading to increased surface resistivity.

CONCLUSIONS

A new class of HIPS-derived antistatic sheets was prepared by compression-molding and extrusion-calendering. Composites with consistent resistivity in the range of 10^5–$10^8\ \Omega$ cm can be prepared by adjusting processing parameters such as re-blending times, compression ratio of screw, and drawing speed in extrusion-calendering. It is advantageous to process sheets with low surface resistivity by choosing extrusion screw with lower compression ratio. On the other hand, it is suggested to fabricate antistatic sheets with slower drawing speed to achieve higher thickness for lower surface resistivity. The mixing process during melt-extrusion is crucial to control the dispersion of SBS and formation of conduction network. Caution needs to be paid in setting processing parameters for large-scale preparation of antistatic sheets with suitable electrical properties.

References

1. Narkis, M.; Lidor, G.; Vaxman, A.; Zuri, L. In Conductive Polymers and Plastics in Industrial Applications. Rupprecht, L., Ed.; Plastic Design Library: Norwich, 1999; p 209.
2. Singh, S. P.; El-Khateeb, H. Packag Technol Sci 1994, 7, 283.
3. Trost, T. Packag Technol Sci 1995, 8, 231.
4. Mohammed, H. A.; Sundararaj, U. Compos A 2008, 39, 284.
5. Kale, V.; Moukwa, M. J Electrost 1996, 38, 239.
6. Dacre, B.; Hetherington, J. I. J Electrost 1998, 45, 53.
7. Huang, J. Adv Polym Technol 2002, 21, 299.
8. Tchoudakov, R.; Breuer, O.; Narkis, M.; Siegmann, A. Polym Eng Sci 1928 1997, 37.
9. Narkis, M.; Lidor, G.; Vaxman, A.; Zuri, L. J Electrost 1999, 47, 201.
10. Hussain, M.; Choa, Y.; Niihara, K. Compos A 2001, 32, 1689.
11. Gubbels, F.; Jerome, R.; Teyssie, P.; Vanlathem, E.; Deltour, R.; Calderone, A.; Parente, V.; Bredas, J. L. Macromolecules 1994, 27, 1972.
12. Gubbels, F.; Blansher, S.; Vanlathem, E.; Jerome, R.; Deltour, R.; Brouers, F.; Teyssie, P. Macromolecules 1995, 28, 1559.
13. Mamunya, Y.; Davydenko, V. V.; Pissis, P.; Lebedev, E. V. Eur Polym Mater 2002, 38, 1887.
14. Ma, C.; Chen, Y.; Kuan, H. J Appl Polym Sci 2005, 98, 2266.
15. Thongruang, W.; Spontak, R. J.; Balik, C. M. Polymer 2002, 43, 2279.
16. Choi, M. H.; Jeon, B. H.; Chung, I. J. Polymer 2000, 41, 3243.

17. Omastová, M.; Chodák, I.; Pionteck, J. Synth Met 1999, 102, 1251.
18. Dhawan, S. K.; Singh, N.; Rodrigues, D. Sci Technol Adv Mater 2003, 4, 105.
19. Petrovic, S.; Martinovic, B.; Divjakovic, V.; Budin-Simendic, J. J Appl Polym Sci 1993, 49, 1659.
20. Andrews, R.; Jacques, D.; Minot, M.; Rantell, T. Macromol Mater Eng 2002, 287, 395.
21. Zhang, J.; Wang, X.; Lu, L.; Li, D.; Yang, X. J Appl Polym Sci 2003, 87, 381.
22. Tang, W.; Tang, J.; Yuan, H.; Jin, R. J Polym Sci Part B Polym Phys 2007, 45, 2136.
23. Tang, J.; Tang, W.; Yuan, H.; Jin, R. J Appl Polym Sci 2007, 104, 4001.
24. Tchoudakov, R.; Breuer, O.; Narkis, M.; Siegmann, A. Polym Eng Sci 1996, 36, 1336.
25. Yi, X.; Wu, G.; Ma, D. J Appl Polym Sci 1998, 67, 131.
26. Tang, J.; Tang, W.; Yuan, H.; Jin, R. J Appl Polym Sci 2010, 115, 190.
27. Tang, W.; Hu, X.; Tang, J.; Jin, R. J Appl Polym Sci 2007, 106, 2648.
28. Asai, S.; Sakata, K.; Sumita, M.; Miyasaka, K. Polym J 1992, 24, 415.
29. Wu, S. Polymer Interface and Adhesion; Marcel Dekker Inc.: NY, 1982.
30. Boonstra, B. B.; Medalia, A.I. Rubber Chem Technol 1963, 36, 15.
31. Dannenberg, E. M. Ind Eng Chem Res 1952, 44, 813.